

Impact of cholesterol on the stability of monomeric and dimeric forms of the translocator protein TSPO: a molecular simulation study

Zeineb Si Chaib^{1,2,*}, Alessandro Marchetto^{3,*}, Klevia Dishnica³, Paolo Carloni^{1,2,4}, Alejandro Giorgetti^{1,3,#}, Giulia Rossetti^{1,5,6#}

¹ Institute for Neuroscience and Medicine (INM-9) and Institute for Advanced Simulations (IAS-5) "Computational biomedicine", Forschungszentrum Jülich, 52425 Jülich, Germany.

² Faculty of Mathematics, Computer Science and Natural Sciences, RWTH Aachen, 52425 Aachen, Germany

³ Department of Biotechnology, University of Verona, 37134 Verona, Italy

⁴ Institute for Neuroscience and Medicine (INM-11) "Molecular Neuroscience and Neuroimaging", Forschungszentrum Jülich, 52425 Jülich

⁵ Jülich Supercomputing Center (JSC), Forschungszentrum Jülich, 52425 Jülich, Germany

⁶ Department of Oncology, Hematology, Oncology, Hemostaseology, and Stem Cell Transplantation University Hospital Aachen, RWTH Aachen University, Pauwelsstraße 30, 52074 Aachen, Germany.

Correspondence: g.rossetti@fz-juelich.de (G.R.), a.giorgetti@fz-juelich.de (A.G.)

* Equally contributed to this work

Supporting Information

Table S1: Overview of the simulated systems.

Simulation	Protein Structure	Bilayer composition	Duration of the MD
<i>m</i> TSPO and <i>m</i> TSPO_mon	2MGY	OMM: 40% POPC, 38.9% SDPE, 14.2% SDPS, 5.9% SAPI, 0.8% CDL2, and CHOL, 10% of total phospholipids Chl_memb: 31% POPC, 41% POPE and 28% CHOL.	8 μ s 8 μ s
<i>m</i> TSPO(Rs) and <i>m</i> TSPO(Rs)_mon	Homology model based on 4UC1	OMM: 40% POPC, 38.9% SDPE, 14.2% SDPS, 5.9%, SAPI, 0.8% CDL2, and CHOL, 10% of total phospholipids) Chl_memb: 31% POPC, 41% POPE and 28% CHOL.	8 μ s 8 μ s
<i>Rs</i> TSPO	4UC3	Rs_memb: 20% POPC, 50% POPE, 24% POPG, 6% CDL2 Chl_memb: 31% POPC, 41% POPE and 28% CHOL.	2 μ s 2 μ s
<i>Bc</i> TSPO	4RYI	Bc_memb: 43%POPE, 40%POPG, 17% CDL2 Chl_memb: 31% POPC, 41% POPE and 28% CHOL.	2 μ s 2 μ s

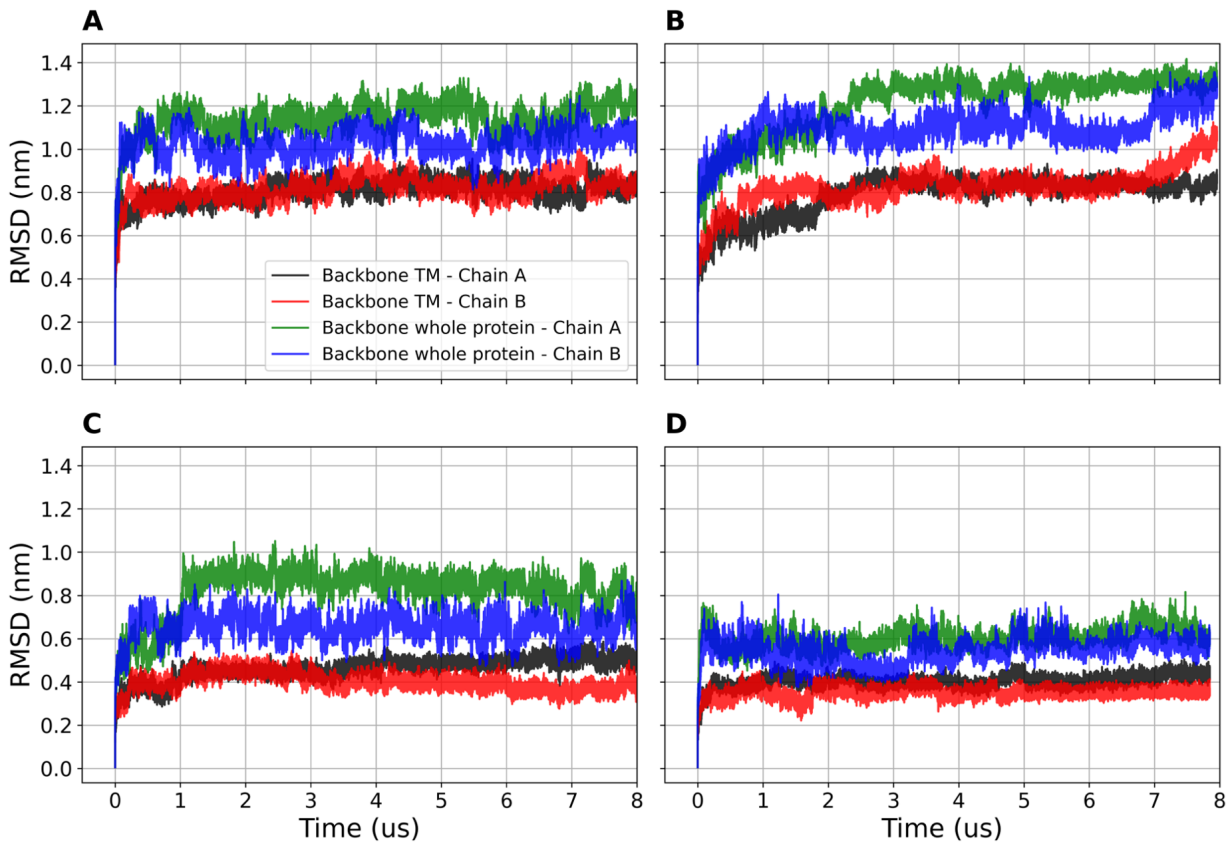


Figure S1. Backbone beads (for a definition of this, see [1]) RMSD of the whole protein and TM regions in **(A)** OMM and **(B)** *chl_mem* for *mTSPO* and in **(C)** OMM and **(D)** *chl_mem* for *mTSPO(Rs)*. The RMSDs are computed with respect to the initial structures in this and all the other figures presented here.

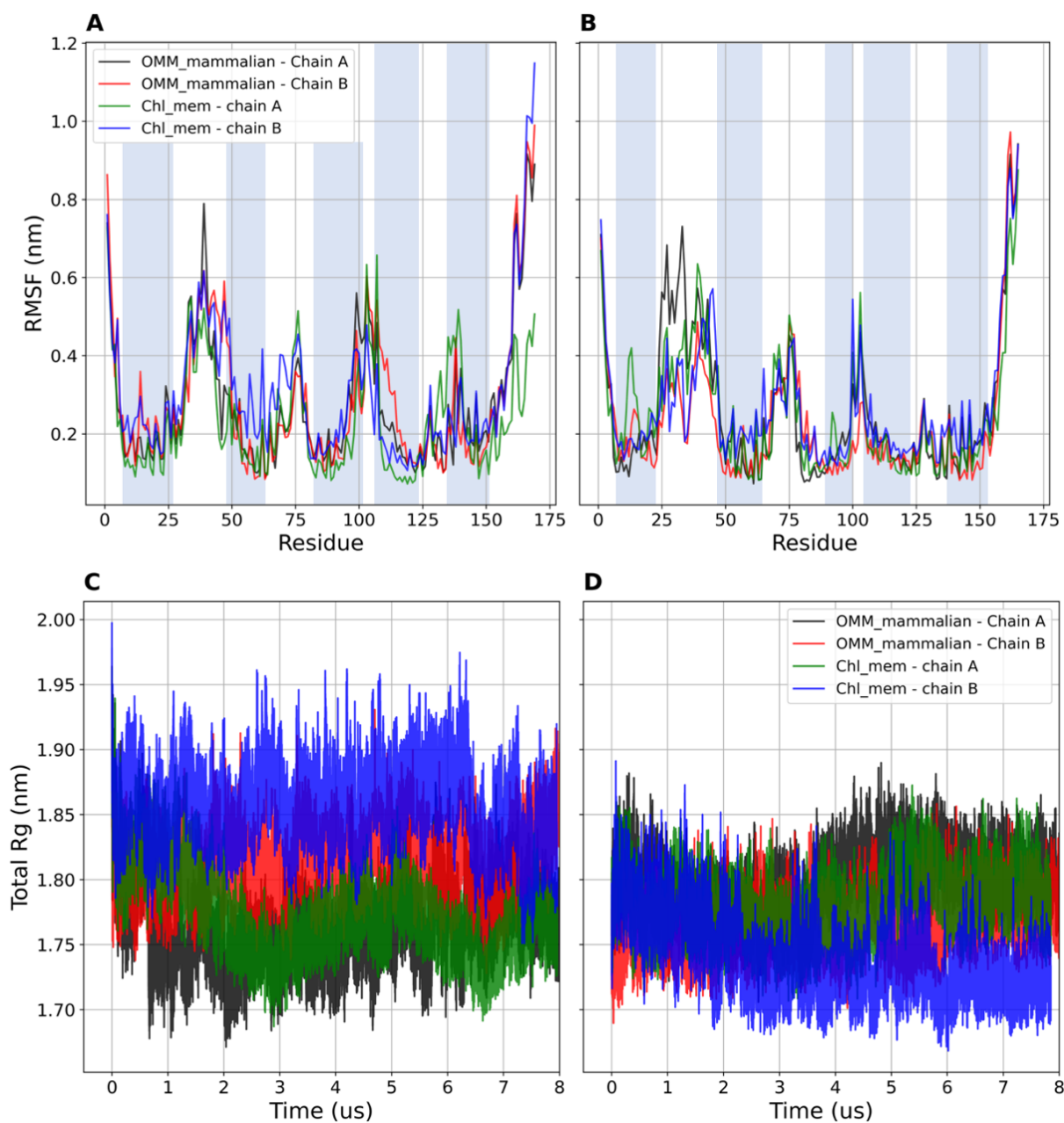


Figure S2. (A-B): RMSF values of each residue in (A) *mTSPO* and (B) *mTSPO*(Rs) embedded in both OMM and chl_mem. The shaded blue regions correspond to the five TMs. The analysis was performed on the equilibrated part of the trajectory, that is for the last 6 μ s. (C-D): The radius of gyration (Rg) is plotted as a function of simulated time for (C) *mTSPO* and (D) *mTSPO*(Rs) embedded in both OMM and chl_mem.

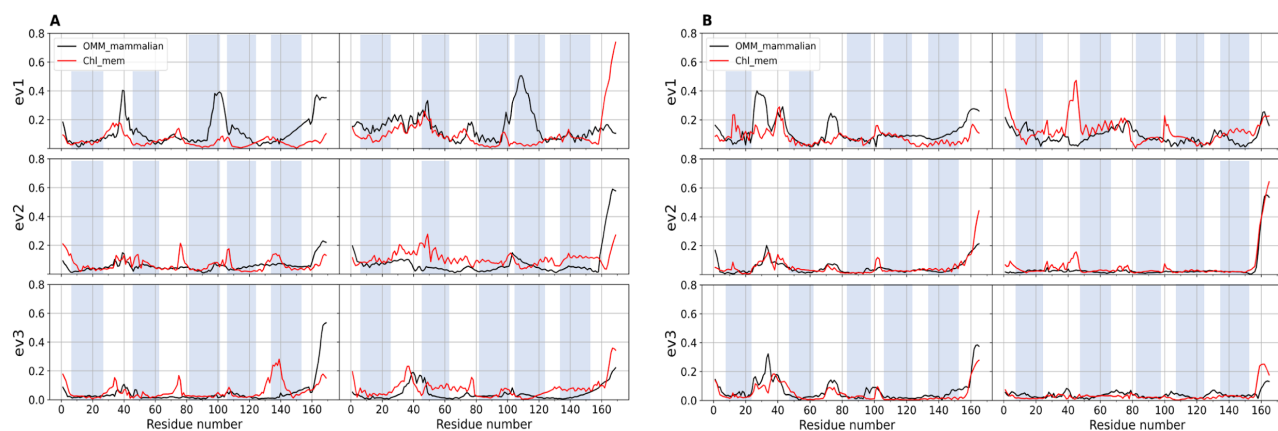


Figure S3. Projection of the backbone beads trajectory along the first three eigenvectors for both chains of **(A)** *mTSPO* and **(B)** *mTSPO*(Rs) dimeric structures. The shaded blue regions correspond to the five TMs. The analysis was performed on the equilibrated part of the trajectory, that is for the last 6 μ s.

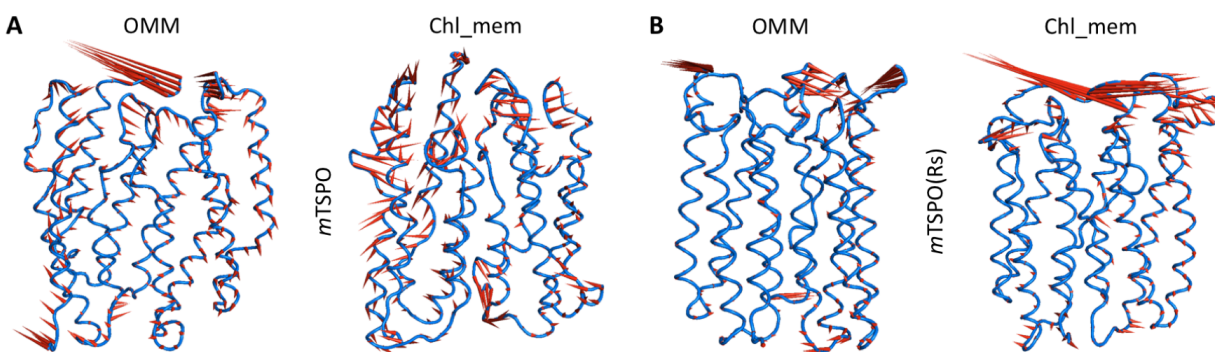


Figure S4. Porcupine plots depicting prominent motions averaged across the second normal mode for: **(A)** *mTSPO*, **(B)** *mTSPO*(Rs) in both OMM and chl_mem. The analysis was performed on the equilibrated trajectory, namely for the last 6 μ s.

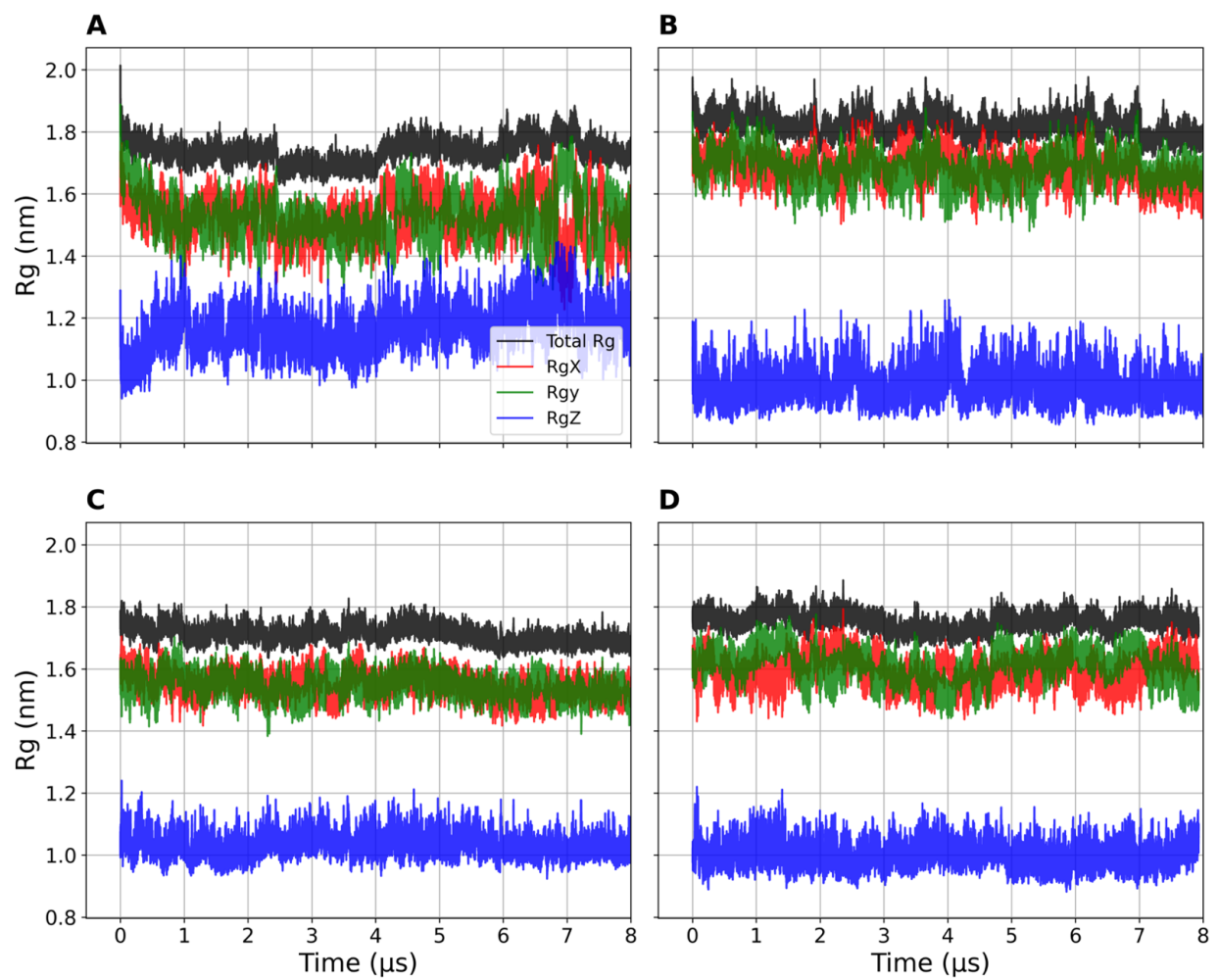


Figure S5. Radius of gyration (Rg) plotted as a function of the simulation time for *mTSPO_mon* in **(A)** OMM and **(B)** chl_mem, as well as for *mTSPO(Rs)_mon* in **(C)** OMM and **(D)** Chl_mem.

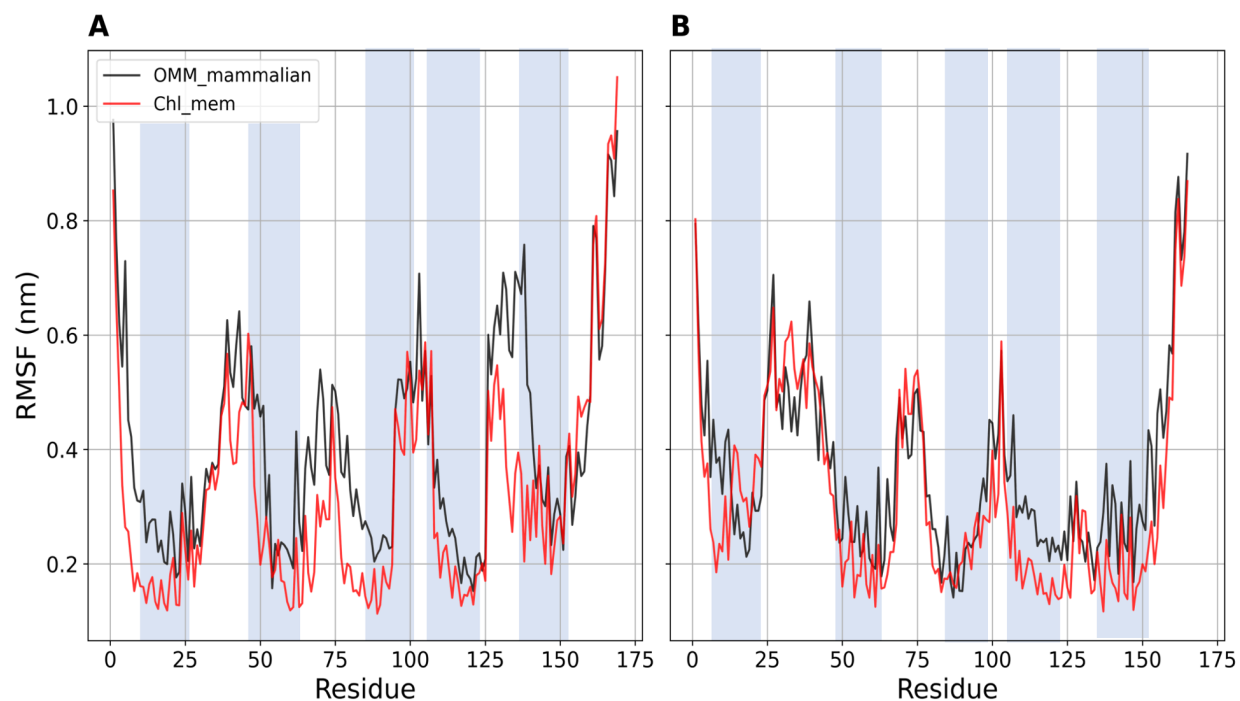


Figure S6. RMSF plots of (A) *mTSPO_mon* and (B) *mTSPO(Rs)_mon* in OMM and chl_mem. The shadowed blue regions correspond to the TMs. The analysis was performed on the equilibrated trajectory, that is for the last 6 μ s.

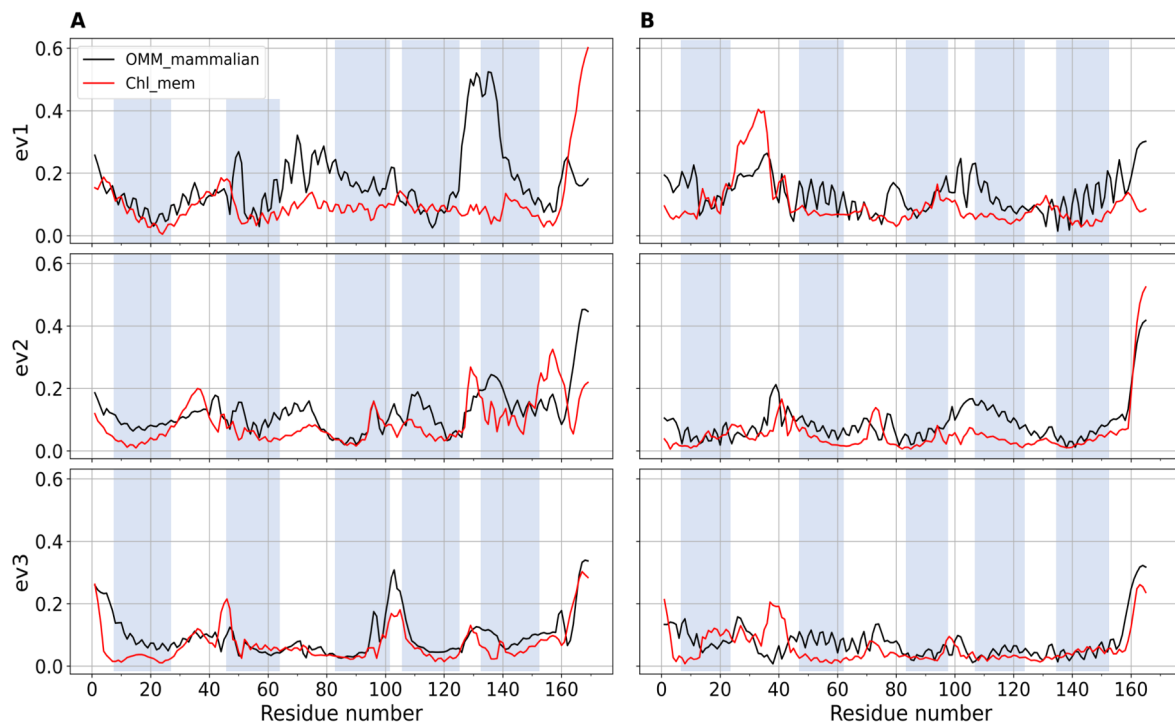


Figure S7. Projection of the backbone beads trajectory along the first three eigenvectors for (A) *mTSPO_mon* and (B) *mTSPO(Rs)_mon*. The shaded blue regions correspond to the five TMs. The analysis was performed on the equilibrated part of the trajectory, that is for the last 6 μ s.

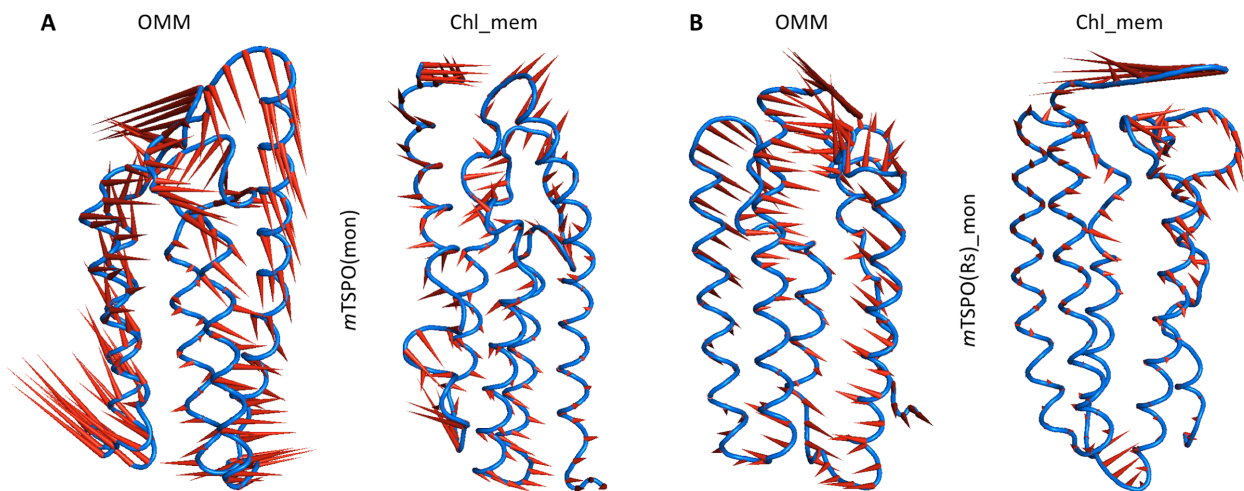


Figure S8. Porcupine plots depicting prominent motions averaged across the second normal mode for (A) *mTSPO_mon* and (B) *mTSPO(Rs)_mon*, in both OMM and chl_mem. The analysis was performed on the equilibrated trajectory, that is for the last 6 μ s.

Bacterial Dimers.

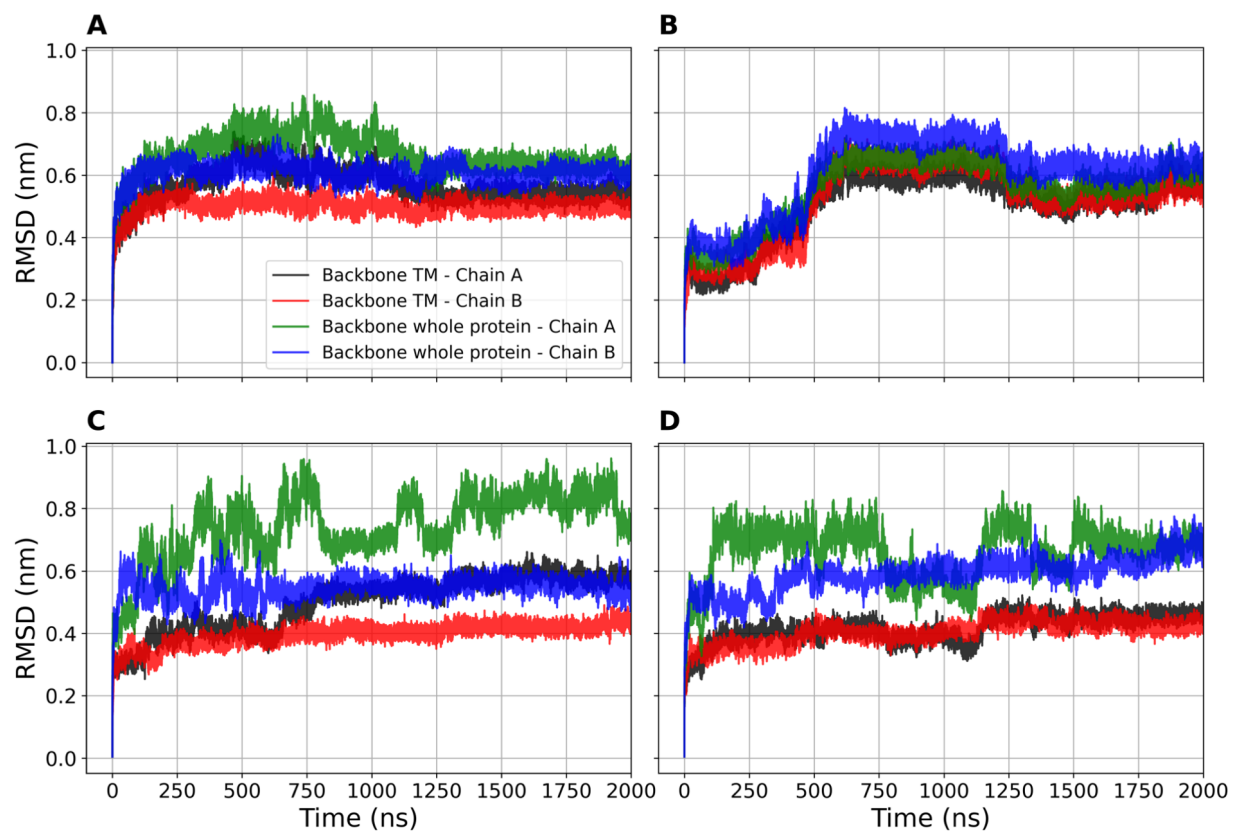


Figure S9. Backbone beads RMSD of the whole protein and TM regions for *BcTSPO* in (A) Bc_mem and (B) chl_mem, as well as for *RsTSPO* in (C) Rs_mem and (D) in chl_mem, plotted as a function of the simulation time.

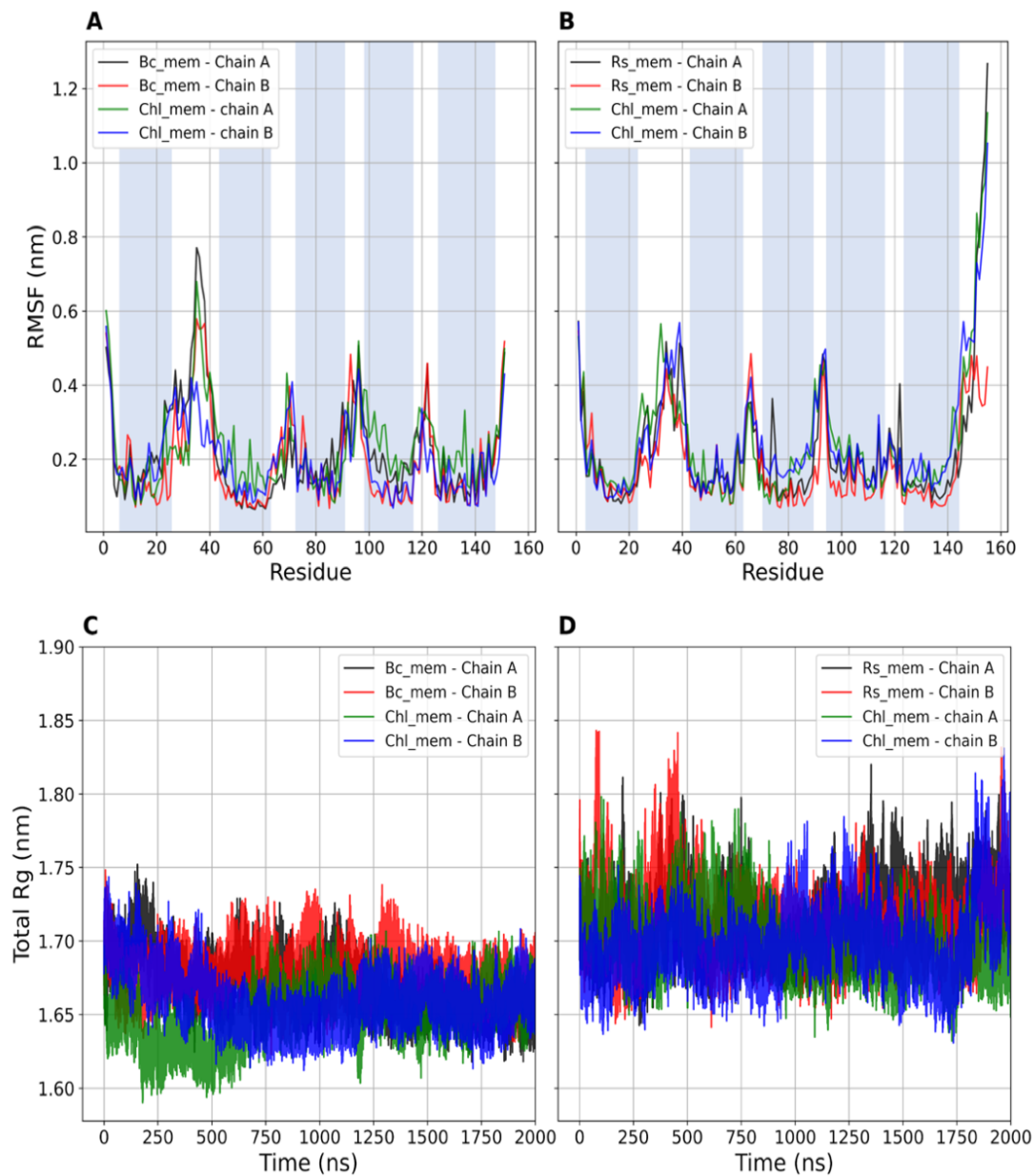


Figure S10. (A-B): RMSF values for each residue in (A) *Bc*TSPO in Bc_mem and chl_mem and (B) *Rs*TSPO in Rs_mem and chl_mem. (C-D): Radius of gyration (Rg) for (C) *Bc*TSPO in Bc_mem and chl_mem and (D) *Rs*TSPO in Rs_mem and chl_mem, plotted as a function of the simulated time. RMSF calculations were performed on the equilibrated part of the trajectories that is, for the last 1.3 μ s.

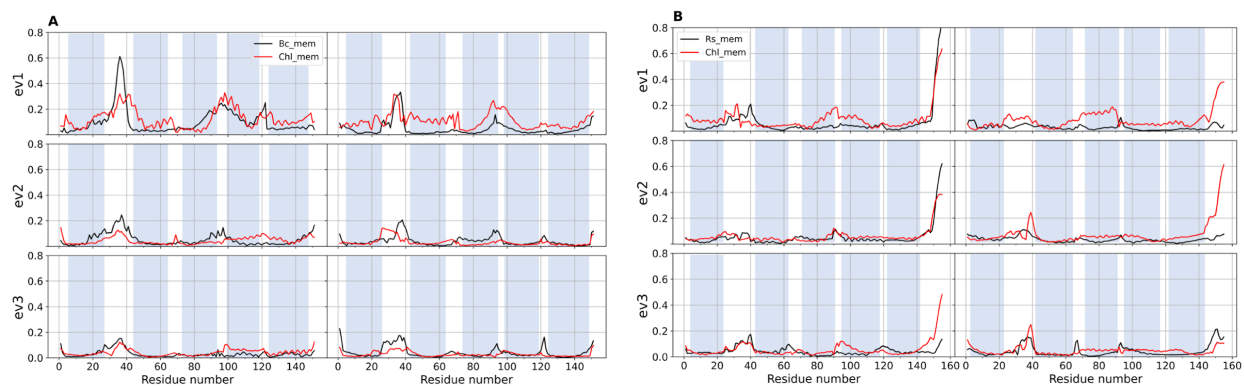


Figure S11. Projection of the backbone beads trajectory along the first three eigenvectors for (A) *BcTSPO* and (B) *RsTSPO*. The blue regions indicate the position of the TMs. The analysis was performed on the equilibrated part of the trajectory, that is, the last 1.3 μ s.

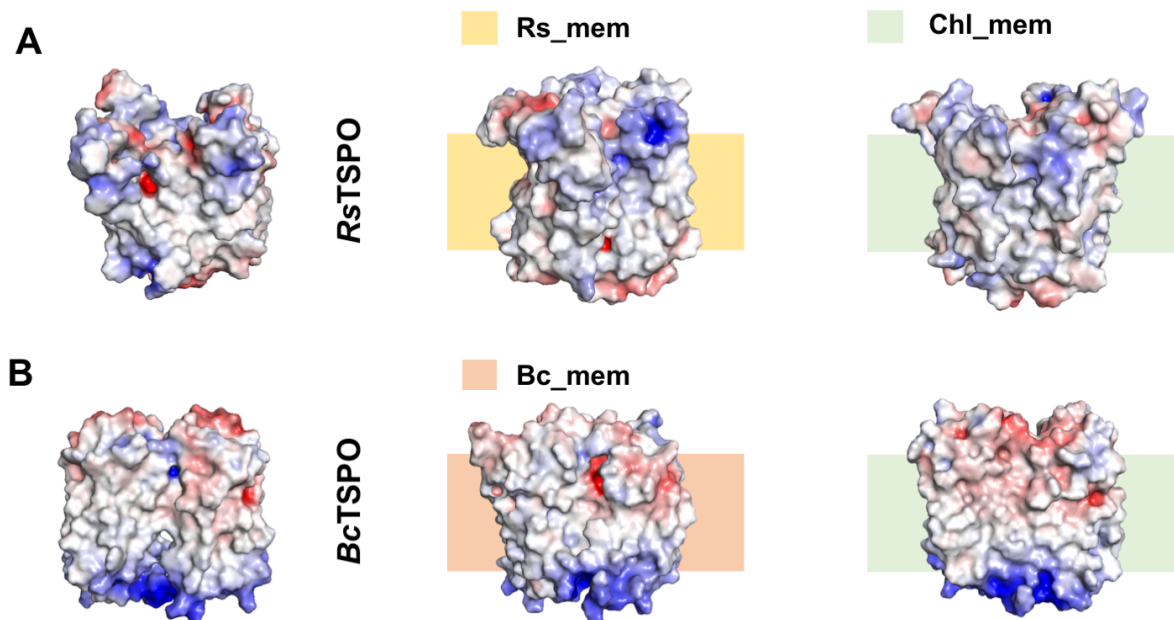


Figure S12. Electrostatic surface potentials in the initial and final MD structures for (A) *RsTSPO* and (B) *BcTSPO* embedded in *Rs_mem*/*Bc_mem* respectively and *chl_mem*. The MD structures were backmapped to all-atom resolution using the backward.py script [2]. The red and blue surfaces represent negative and positive electrostatic potentials, respectively. The maximum values of the potentials are -5 kT/e, +5kT/e, respectively. Red and blue surfaces represent negative and positive electrostatic potentials (-5 kT/e, +5kT/e), respectively.

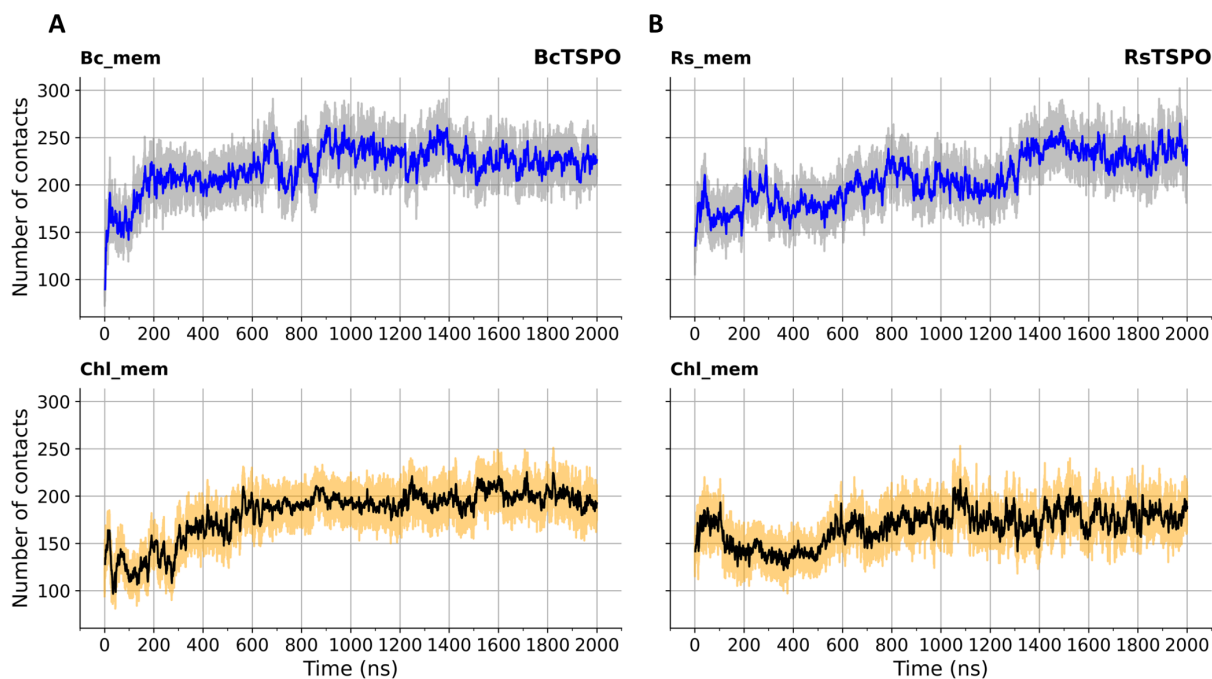


Figure S13. Number of subunit-subunit contact beads plotted as a function of the simulation time for **(A)** *BcTSPO* in *Bc_mem* and *chl_mem* and **(B)** *RsTSPO* in *Rs_mem* and *chl_mem*. For the definition of the contacts, see Methods Section in the main text.

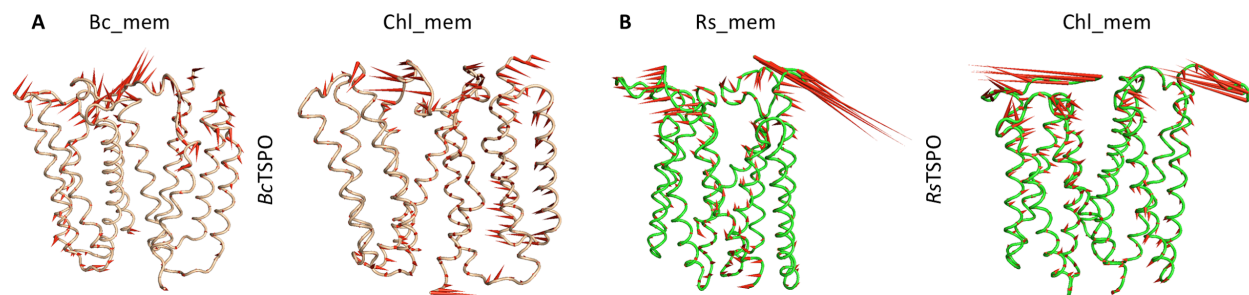


Figure S14. Porcupine plots depicting large scale motions averaged across the second normal mode for **(A)** *BcTSPO* embedded in *Bc_mem* and *chl_mem* and **(B)** *RsTSPO* embedded in *Rs_mem* and *chl_mem*. The analysis was performed on the equilibrated trajectory, that is for the last 1.3 μ s.

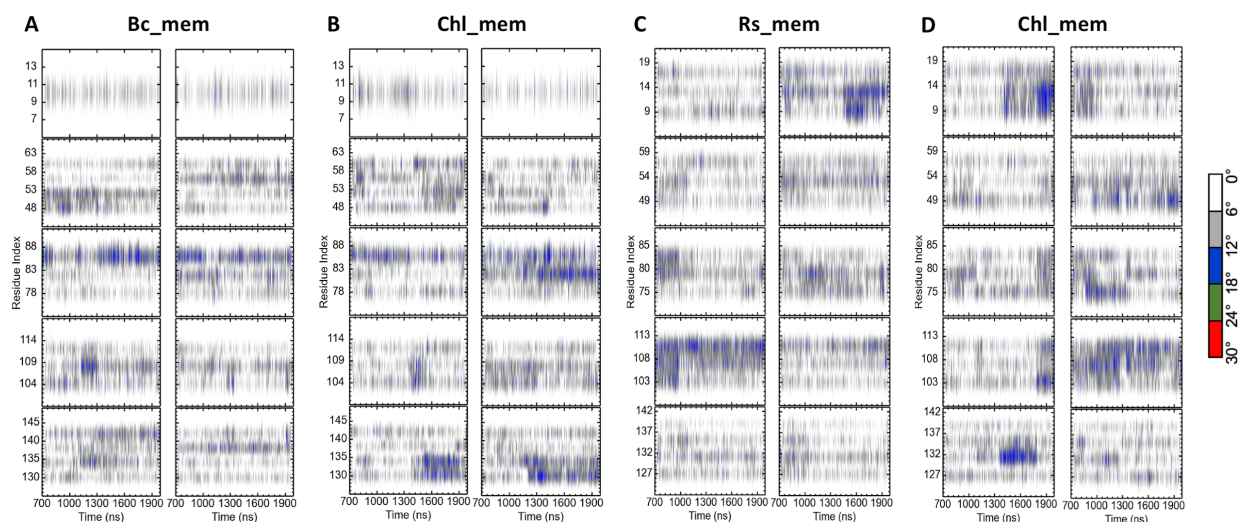


Figure S15. Helix bending of BcTSPO embedded in (A) Bc_mem, (B) chl_mem and for RsTSPO in (C) Rs_mem and (D) chl_mem, plotted as a function of the simulation time. The analysis was performed on the equilibrated part of the trajectories, that is, the last 1.3 μ s.

References

1. de Jong, D.H.; Singh, G.; Bennett, W.D.; Amarez, C.; Wassenaar, T.A.; Schäfer, L.V.; Periole, X.; Tieleman, D.P.; Marrink, S.J. Improved parameters for the martini coarse-grained protein force field. *Journal of chemical theory and computation* **2013**, *9*, 687-697.
2. Wassenaar, T.A.; Pluhackova, K.; Böckmann, R.A.; Marrink, S.J.; Tieleman, D.P. Going backward: a flexible geometric approach to reverse transformation from coarse grained to atomistic models. *Journal of chemical theory and computation* **2014**, *10*, 676-690.